

# Macrocyclic $\beta$ -sheet mimics that antagonize protein aggregation and reduce amyloid toxicity

Pin-Nan Cheng<sup>1†</sup>, Cong Liu<sup>2†</sup>, Minglei Zhao<sup>2</sup>, David Eisenberg<sup>2\*</sup> and James S. Nowick<sup>1\*</sup>

The amyloid protein aggregation associated with diseases such as Alzheimer's, Parkinson's and type II diabetes (among many others) features a bewildering variety of  $\beta$ -sheet-rich structures from native proteins to ordered oligomers and fibres. The variation in the amino-acid sequences of the  $\beta$ -structures presents a challenge to developing a model system of  $\beta$ -sheets for the study of various amyloid aggregates. Here, we introduce a family of robust  $\beta$ -sheet macrocycles that can serve as a platform to display a variety of heptapeptide sequences from different amyloid proteins. We have tailored these amyloid  $\beta$ -sheet mimics (ABSMs) to antagonize the aggregation of various amyloid proteins, thereby reducing the toxicity of amyloid aggregates. We describe the structures and inhibitory properties of ABSMs containing amyloidogenic peptides from the amyloid- $\beta$  peptide associated with Alzheimer's disease,  $\beta_2$ -microglobulin associated with dialysis-related amyloidosis,  $\alpha$ -synuclein associated with Parkinson's disease, islet amyloid polypeptide associated with type II diabetes, human and yeast prion proteins, and Tau, which forms neurofibrillary tangles.

Amyloid aggregation is associated with many intractable protein aggregation diseases, notably including Alzheimer's disease, Huntington's disease, Parkinson's disease, type II diabetes and prion diseases<sup>1–3</sup>. Amyloid fibrils with characteristic highly ordered cross- $\beta$  structures are the ultimate products of amyloid aggregation. More than 30 proteins have been linked to amyloidogenesis, and they demonstrate enormous variations in relation to their sequences and polymorphic fibril structures<sup>4–6</sup>. The fibril formation of a given polypeptide, however, greatly depends on its specific residue order<sup>7,8</sup>. Crystallographic structures of amyloid-like fibrils formed by amyloidogenic peptide fragments suggest that the formation of highly ordered parallel or antiparallel  $\beta$ -sheets and a steric zipper interface between  $\beta$ -sheets are two essential elements for amyloid fibril formation<sup>9,10</sup>.

Amyloid fibrils are the most visible evidence of pathology, but soluble oligomers are proving to be more important in amyloid toxicity<sup>11,12</sup>. Although there is an increasing level of evidence showing that these transient, unstable structures are rich in  $\beta$ -sheets, their dynamic and polymorphic properties make amyloid oligomers difficult to study at the atomic level<sup>13–15</sup>. Additional tools are needed to study amyloid oligomers and aggregation and to shed light on controlling these processes.

$\beta$ -Sheet mimics that can display amyloid  $\beta$ -strands provide a means with which to study amyloid oligomers and aggregation. We previously introduced 42-membered ring macrocyclic  $\beta$ -sheets containing pentapeptide fragments from amyloid- $\beta$  peptide (A $\beta$ ) and tau protein (Tau) to mimic amyloid-like  $\beta$ -sheets and shed light on the structures of transient amyloid oligomers<sup>16,17</sup>. We have also used these macrocyclic  $\beta$ -sheets to inhibit aggregation of the peptide Ac-VQIVYK-NH<sub>2</sub> (AcPHF6), derived from Tau, to provide insights into the aggregation process<sup>18</sup>.

The development of a robust chemical model of  $\beta$ -sheets that can tolerate a variety of amino-acid sequences has been challenging, because amyloidogenic sequences vary enormously and because folding of  $\beta$ -sheet mimics largely depends on the amino-acid sequence<sup>1,19</sup>. In this Article, we introduce a new class of  $\beta$ -sheet

macrocycles that can tolerate a wide range of amino-acid sequences from amyloid proteins and still fold into  $\beta$ -sheet structures. We call these macrocycles amyloid  $\beta$ -sheet mimics (ABSMs).

ABSM 1 is a 54-membered ring, comprising a heptapeptide  $\beta$ -strand (the upper strand), one Hao unit flanked by two dipeptides (the lower strand) and two  $\delta$ -linked ornithine ( $\delta$ Orn) turns (Fig. 1a). The 'upper'  $\beta$ -strand of ABSM 1 incorporates different heptapeptide fragments from A $\beta$ , Tau, yeast Sup35 prion protein (Sup35), human prion protein (hPrP), human  $\beta_2$ -microglobulin (h $\beta_2$ M), human  $\alpha$ -synuclein (h $\alpha$ Syn) and human islet amyloid

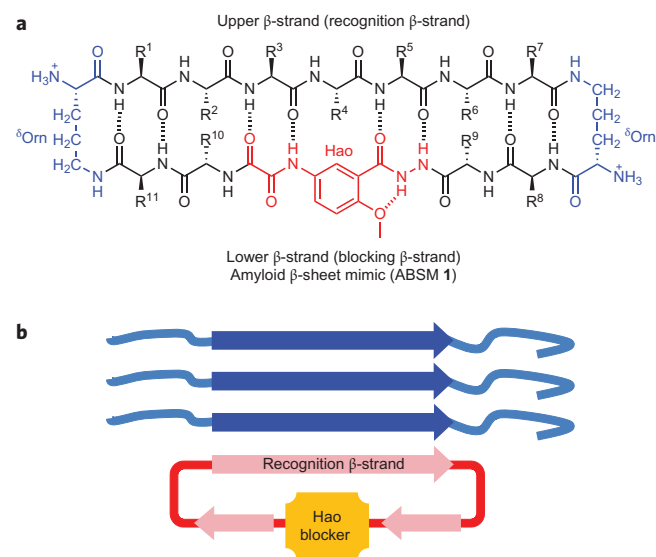


**Figure 1 | Design of ABSM 1.** **a**, Representation of ABSM 1 illustrating the upper  $\beta$ -strand (recognition  $\beta$ -strand), the  $\delta$ -linked ornithine ( $\delta$ Orn) turn unit and the Hao amino-acid blocker unit. **b**, Representation of ABSM 1 recognizing and blocking amyloid aggregation through  $\beta$ -sheet interactions.

<sup>1</sup>Department of Chemistry, University of California, Irvine, California 92697-2025, USA, <sup>2</sup>UCLA-DOE Institute for Genomics and Proteomics, Howard Hughes Medical Institute, Molecular Biology Institute, University of California, Los Angeles, California, 90095-1570, USA, <sup>†</sup>These authors contributed equally to this work. \*e-mail: jsnowick@uci.edu; david@mbi.ucla.edu

1 polypeptide (hIAPP). Hao is a tripeptide  $\beta$ -strand mimic that not  
2 only serves as a template for intramolecular hydrogen bonding,  
3 but also minimizes the exposed hydrogen-bonding functionality  
4 of the 'lower' strand<sup>20</sup>. This structural design of Hao helps prevent  
5 ABSMs **1** from aggregating in solution to form an infinite  
6 network of  $\beta$ -sheets; instead, ABSMs **1** dimerize and then further  
7 self-assemble into oligomers. The 'upper' and 'lower' strands of  
8 ABSM **1** are connected by two  $\delta$ Orn  $\beta$ -turn mimics<sup>21</sup>.

9 We envisioned that ABSM **1** would fold well because it is confor-  
10 mationally constrained by cyclicity and has a Hao template to  
11 promote intramolecular hydrogen bonding and two  $\delta$ Orn  $\beta$ -turn  
12 mimics to promote turn formation. We also envisioned that four  
13 pairs of side chains ( $R_1$ - $R_{11}$ ,  $R_2$ - $R_{10}$ ,  $R_6$ - $R_9$  and  $R_7$ - $R_8$ ) would  
14 provide stabilizing transannular interactions. We anticipated that  
15 the flexibility of the dipeptides flanking Hao in the 'lower' strand  
16 would better accommodate the flatness of the Hao template and  
17 thus minimize the kinks in the  $\beta$ -strands that we had previously  
18 observed in 42-membered ring macrocycles<sup>17</sup>.

19 We designed ABSMs **1** to display exposed heptapeptide  
20  $\beta$ -strands so that these  $\beta$ -strands can recognize and bind their  
21 parent amyloid proteins (Fig. 1b). We envisioned recognition  
22 between ABSMs **1** and their parent amyloid proteins to take place  
23 through the  $\beta$ -sheet interactions observed in amyloid aggregation.  
24 Here, we present structural studies of these ABSMs **1** and describe  
25 their effect upon amyloid aggregation and toxicity.

## 26 Results

27 **Design of ABSMs 1.** To test the folding of ABSMs **1**, we selected 16  
28 amyloidogenic heptapeptide  $\beta$ -strands from seven  $\beta$ -sheet-rich  
29 amyloid proteins for positions 1–7 in the 'upper' strands  
30 (Table 1). ABSMs **1a–g** contain heptapeptide sequences from two  
31 important hydrophobic and fibril-forming regions of A $\beta$   
32 associated with Alzheimer's disease, residues 16–23 and 29–40  
33 (refs 5,22). ABSMs **1a–d** and **f** contain native heptapeptide  
34 sequences, while ABSMs **1e** and **1g** are G33F and G37F mutants,  
35 in which the aromatic residue across from Hao promotes better  
36 folding<sup>16</sup>. ABSM **1h** contains residues 7–13 from Sup35, which  
37 has been widely used as a model to study amyloid formation<sup>9</sup>.  
38 ABSM **1i** contains residues 116–122 from hPrP, which is the  
39 infectious agent of prion diseases<sup>23</sup>. ABSM **1j** contains residues  
40 305–311 from Tau, which forms neurofibrillary tangles<sup>24</sup>. ABSM  
41 **1k–m** contain residues 62–68 and 63–69 from h $\beta_2$ M, which is

42 associated with dialysis-related amyloidosis<sup>25</sup>. ABSMs **1n** and **1o**  
43 contain residues 69–75 and 75–81 from h $\alpha$ Syn, which is  
44 associated with Parkinson's disease<sup>26</sup>. ABSMs **1p** and **1q** contain  
45 residues 11–17 and 26–32 from hIAPP, associated with type II  
46 diabetes<sup>27</sup>. We chose polar and hydrophobic residues at positions  
47 8–11 in the 'lower' strands of ABSMs **1** to promote solubility in  
48 water and to increase hydrophobic residues that favour  
49  $\beta$ -sheet formation.

**Synthesis of ABSMs 1.** ABSMs **1** were prepared by synthesizing the  
50 corresponding protected linear peptides, followed by solution-phase  
51 cyclization and deprotection<sup>28</sup>. The protected linear peptide  
52 precursors were synthesized on 2-chlorotrityl chloride resin by  
53 conventional Fmoc-based solid-phase peptide synthesis.  
54 Macrocyclization was typically performed using HCTU and  
55 *N,N*-diisopropylethylamine in DMF at a concentration of  
56 ~0.5 mM. The ABSMs **1** were isolated in ~20–30% overall yield  
57 after high-performance liquid chromatography purification and  
58 lyophilization. Each synthesis produces tens of milligrams of  
59 ABSMs **1** as fluffy white solids (for details, see Supplementary  
60 Information).  
61

**X-ray crystallographic studies of ABSM 1r.** X-ray crystallography  
62 of ABSM **1r** validated the design of ABSMs **1** (Fig. 2). ABSM **1r** is a  
63 homologue of ABSM **1d**, with the Tyr residue in the 'lower' strand  
64 replaced with 4-bromophenylalanine for crystallographic phase  
65 determination. ABSM **1r** adopts a  $\beta$ -sheet structure in which the  
66 'upper' and 'lower' strands are intramolecularly hydrogen-bonded  
67 to form eight hydrogen bonds (Fig. 2a). The two  $\delta$ Orn residues of  
68 ABSM **1r** fold into  $\beta$ -turn-like conformations, Hao mimics a  
69 tripeptide  $\beta$ -strand, and the 'upper' strand displays an exposed  
70 heptapeptide  $\beta$ -sheet edge.  
71

72 ABSM **1r** forms a dimer in the crystal lattice in which the two  
73 recognition  $\beta$ -strands come together in an antiparallel  $\beta$ -sheet  
74 fashion (Fig. 2b). The  $\beta$ -strands of the dimerization interface are  
75 shifted out of register, forming only six hydrogen bonds instead of  
76 the eight that would form through in-register contact.

77 The dimers stack in the crystal lattice, with hydrophobic contacts  
78 between the layers of the stack. The Ile, Leu and Val, at positions 3, 5  
79 and 7 on the 'top' face of the dimer pack, are together in one set of  
80 hydrophobic contacts 'above' the dimer, while the Met and Phe at  
81 positions 6 and 9 on the 'bottom' face of the dimer pack are together  
82 in another set of hydrophobic contacts 'below' the dimer (Fig. 2c,d).

**Table 1 | Amino acid sequences and key NOEs of ABSMs 1a–q.**

	Sequence	$R_1$ - $R_7$	$R_8$ - $R_{11}$	Orn $_{\alpha-\delta S}$	2-10	4-Hao $_6$	6-9	Orn $_{\alpha-\delta S}$	Folding
<b>1a</b>	A $\beta_{16-22}$	KLVFFAE	KLIE	S*	— <sup>†</sup>	S	S	S	Good
<b>1b</b>	A $\beta_{17-23}$	LVFFAED	KLIE	S	S	S	S	S	Good
<b>1c</b>	A $\beta_{29-35}$	GAIIGLM	KFYK	S	S	S	S	S	Good
<b>1d</b>	A $\beta_{30-36}$	AIIGLMV	KFYK	S	S	S	S	S	Good
<b>1e</b>	A $\beta_{30-36}$ G33F	AIIFLMV	KFYK	S	S	S	S	S	Good
<b>1f</b>	A $\beta_{34-40}$	LMVGGVV	KFYK	S	S	W*	— <sup>‡</sup>	S	Moderate
<b>1g</b>	A $\beta_{34-40}$ G37F	LMVFGVV	KFYK	S	S	S	S	S	Good
<b>1h</b>	Sup35 $_{7-13}$	GQQNNQY	KFYK	W	— <sup>‡</sup>	— <sup>‡</sup>	— <sup>‡</sup>	W	Poor
<b>1i</b>	hPrP $_{116-122}$	AAAGAVV	KFYK	W	W	— <sup>‡</sup>	— <sup>‡</sup>	W	Poor
<b>1j</b>	Tau $_{305-311}$	SVQIVYK	EFYK	S	S	S	S	S	Good
<b>1k</b>	h $\beta_2$ M $_{62-68}$	FYLLYYT	KNSA	S	S	S	— <sup>†</sup>	S	Good
<b>1l</b>	h $\beta_2$ M $_{63-69}$	YLLYYTE	FKVS	W	— <sup>‡</sup>	— <sup>‡</sup>	— <sup>‡</sup>	W	Poor
<b>1m</b>	h $\beta_2$ M $_{63-69}$	YLLYYTE	KVVK	S	— <sup>§</sup>	S	— <sup>§</sup>	S	Good
<b>1n</b>	h $\alpha$ Syn $_{69-75}$	AVVTGVT	KFYK	S	S	S	— <sup>§</sup>	S	Good
<b>1o</b>	h $\alpha$ Syn $_{75-81}$	TAVANKT	VFYK	S	S	S	— <sup>§</sup>	S	Good
<b>1p</b>	hIAPP $_{11-17}$	RLANFLV	KFYK	S	S	S	S	S	Good
<b>1q</b>	hIAPP $_{26-32}$	ILSSTNV	KFYK	S	S	S	S	S	Good
<b>1r</b>	A $\beta_{30-36}$	AIIGLMV	KFF <sup>Br</sup> K						

\*S, strong NOE; W, weak NOE. <sup>†</sup>NOE not observed due to overlap of proton resonances. <sup>‡</sup>NOE not observed. <sup>§</sup>NOE not observable due to overlap with HOD.

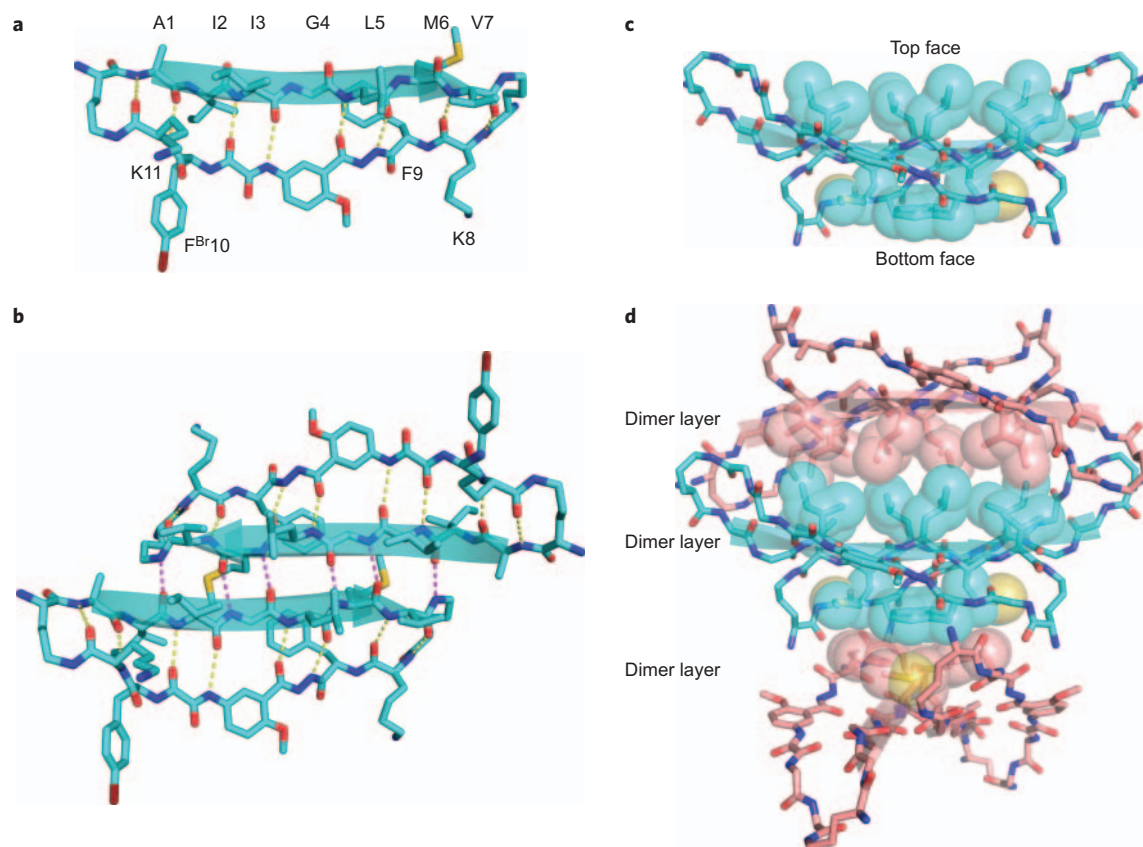


**Figure 2 | X-ray crystallographic structure of ABSM 1r, which contains the heptapeptide sequence AIIGLMV ( $A\beta_{30-36}$ ).** **a**, The monomer. **b,c**, The dimer (top view, **b**; side view, **c**). **d**, Stacked layers of dimer in the crystal lattice. Note that the view in **b** is perpendicular to the  $\beta$ -sheet (top view), whereas the view in **c** and **d** is  $90^\circ$  away, parallel to the  $\beta$ -sheet (side view), and shows the hydrophobic contacts. Some side chains in **c** and **d** have been omitted for clarity.

1 The hydrophobic contacts between the dimer layers appear to be  
 2 important in the crystallization and supramolecular assembly of  
 3 ABSM 1r and may explain the formation of the out-of-register inter-  
 4 face within the dimer.

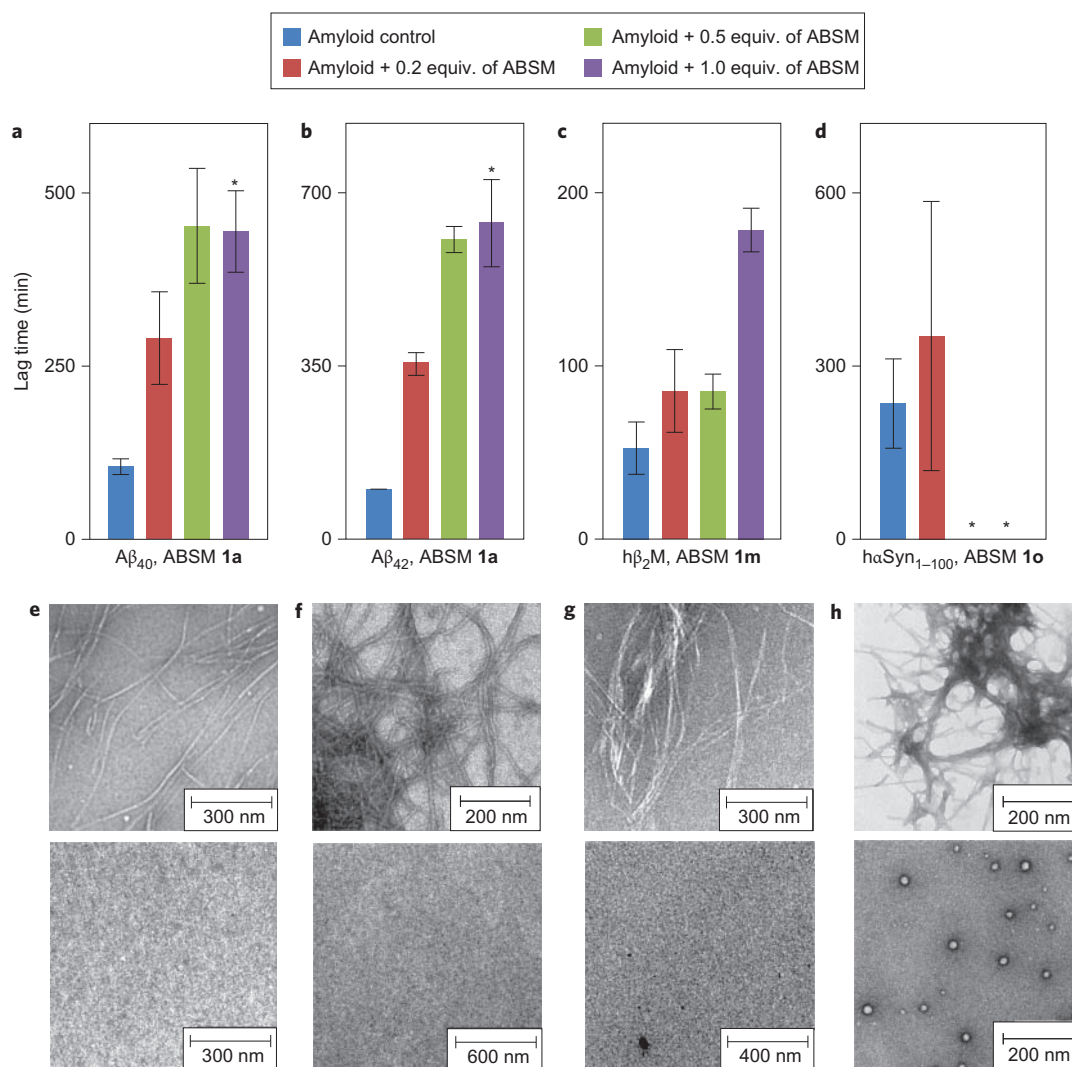
5  **$^1\text{H}$  NMR studies of ABSMs 1.**  $^1\text{H}$  NMR studies of ABSMs 1a–q in  
 6  $\text{D}_2\text{O}$  solution further validated the design of ABSMs 1 and  
 7 established that ABSMs 1 generally adopted folded  $\beta$ -sheet  
 8 structures in solution. The  $^1\text{H}$  NMR spectra of ABSMs 1 show  
 9 sharp, disperse resonances at submillimolar and low millimolar  
 10 concentrations in  $\text{D}_2\text{O}$  solution, suggesting ABSMs 1 to be non-  
 11 aggregating in water. Antiparallel  $\beta$ -sheets have close contacts  
 12 between the  $\alpha$ -protons of the non-hydrogen-bonded pairs of  
 13 amino acids, which generally demonstrate strong interstrand  
 14 nuclear Overhauser effect cross-peaks (NOEs). In ABSMs 1, these  
 15 close contacts should involve the  $\alpha$ -protons of residues 2 and 10  
 16 (2–10) and residues 6 and 9 (6–9). There should also be  
 17 homologous contacts involving the  $\alpha$ -proton of residue 4 and  $\text{H}_\alpha$   
 18 of Hao (4–Hao $_6$ ) and the  $\alpha$ - and *pro-S*  $\delta$ -protons of the  $^{\delta}\text{Orn}$   
 19 turns ( $\text{Orn}_{\alpha-\delta\text{S}}$ ). Table 1 shows these contacts.

20 All ABSMs, except 1h, 1i and 1l, exhibit most of these key NOEs  
 21 (Table 1). ABSMs 1a–e, 1g, 1j, 1k and 1m–q show strong 2–10, 6–9,  
 22 4–Hao $_6$  and  $\text{Orn}_{\alpha-\delta\text{S}}$  NOEs and thus exhibit good folding. ABSM 1f  
 23 shows strong  $\text{Orn}_{\alpha-\delta\text{S}}$  and 2–10 NOEs and a weak 4–Hao $_6$  NOE,  
 24 and therefore exhibits moderate folding. ABSMs 1h, 1i and  
 25 1l show only  $\text{Orn}_{\alpha-\delta\text{S}}$  NOEs and thus exhibit weak  
 26 folding. Although the lack of the interstrand NOEs indicates poor  
 27 folding of ABSMs 1h, 1i and 1l, the  $\text{Orn}_{\alpha-\delta\text{S}}$  NOEs suggest that  
 28 their  $^{\delta}\text{Orn}$  residues fold at least partially into a  $\beta$ -turn-like

conformation. Table 1 summarizes the observed key NOEs and  
 the folding of ABSMs 1.

**Inhibition of amyloid aggregation by ABSMs 1.** Thioflavin T  
 (ThT) fluorescence assays and transmission electron microscopy  
 (TEM) studies showed that the ABSMs containing amyloidogenic  
 sequences can inhibit the aggregation of amyloid proteins. We  
 studied the inhibition of  $A\beta_{40}$  and  $A\beta_{42}$  aggregation by ABSM 1a,  
 the inhibition of  $h\beta_2\text{M}$  aggregation by ABSM 1m and the  
 inhibition of truncated human  $\alpha$ -synuclein ( $h\alpha\text{Syn}_{1-100}$ )  
 aggregation by ABSM 1o.

ThT fluorescence assays show that ABSMs 1a, 1m and 1o effectively  
 delay aggregation of their parent proteins at sub-stoichiometric  
 concentrations in a dose-dependent manner (Fig. 3a–d).  
 At 0.2 equiv., ABSM 1a delays  $A\beta_{40}$  and  $A\beta_{42}$  aggregation by  
 280% and 350%, respectively, and at 0.5 equiv. by 430 and 600%  
 (Fig. 3a,b). Although ThT fluorescence assays show that  $A\beta$   
 aggregation exhibits comparable lag times at 0.5 and 1.0 equiv. of  
 ABSM 1a, the growth phases of the aggregation are much slower at  
 1.0 equiv. than at 0.5 equiv. (asterisks in Fig. 3a,b; for details, see  
 Supplementary Figs S1 and S2). ABSM 1m delays  $h\beta_2\text{M}$  aggregation  
 by 160% at 0.2 and 0.5 equiv. and by 340% at 1.0 equiv. (Fig. 3c).  
 ABSM 1o delays  $h\alpha\text{Syn}_{1-100}$  aggregation by 150% at 0.2 equiv.  
 (Fig. 3d). Although  $h\alpha\text{Syn}_{1-100}$  aggregation exhibits longer lag  
 times with 0.5 and 1.0 equiv. of ABSM 1o than with 0.2 equiv.,  
 some runs showed complete suppression of aggregation, and yet  
 other runs showed typical sigmoidal curves. Because of this  
 scatter in the data, precise lag times are not reported (asterisk in  
 Fig. 3d; for details see Supplementary Fig. S4.) TEM studies of



1 samples taken directly from the ThT assays show that  $A\beta$ ,  
 2  $h\beta_2M$  and  $h\alpha Syn_{1-100}$  form fibrils without ABSMs and do  
 3 not form fibrils with ABSMs (1.0 equiv.) during the delayed lag  
 4 time (Fig. 3e–h).

5  $A\beta$  has been shown to cross-interact with different amyloido-  
 6 genic proteins containing similar primary sequences<sup>29–31</sup>. To inves-  
 7 tigate cross-interaction of  $A\beta$  with ABSMs, we compared the  
 8 interaction of  $A\beta$  with ABSM **1a** to that with ABSM **1m**, which  
 9 has a closely homologous sequence, and to that with ABSM **1o**,  
 10 which does not (Supplementary Fig. S5). ThT fluorescence  
 11 assays show that ABSM **1m** inhibits  $A\beta$  aggregation, like  
 12 ABSM **1a**, whereas ABSM **1o** has little or no inhibitory  
 13 effect (Supplementary Fig. S5). This result suggests that  
 14 structurally homologous ABSMs can not only interact with their  
 15 parent amyloid proteins but can also cross-interact with different  
 16 amyloid proteins.

To further investigate the effect of sequence on inhibition, we  
 compared the interaction of ABSM **1a** with  $A\beta_{40}$  to that of  
 ABSMs **1b**, **1c**, **1d** and **1f** with  $A\beta_{40}$ . ThT fluorescence assays  
 show that ABSM **1b** is effective against  $A\beta_{40}$  aggregation, whereas  
 ABSMs **1c**, **1d** and **1f** cause little or no inhibition (Supplementary  
 Fig. S6). The inhibition of  $A\beta_{40}$  aggregation by both ABSMs **1a**  
 and **1b** indicates that the central hydrophobic sequence  $A\beta_{17-21}$  is  
 critical to the activity of ABSMs against  $A\beta_{40}$  aggregation. This  
 result supports the role of  $A\beta_{17-21}$  in  $A\beta$  aggregation and suggests  
 that strong interaction of this sequence in these ABSMs with that  
 of the  $A\beta$  oligomers delays  $A\beta$  aggregation<sup>22,32</sup>.

**Detoxification of  $A\beta$  by ABSM **1a**.** Cell viability (MTT) assays  
 established that ABSM **1a** reduces the toxicity of  $A\beta_{40}$  and  $A\beta_{42}$   
 in PC-12 cells (Fig. 4) and that ABSMs **1a**, **1m** and **1o** exhibit  
 little or no toxicity (Supplementary Fig. S9). We examined the

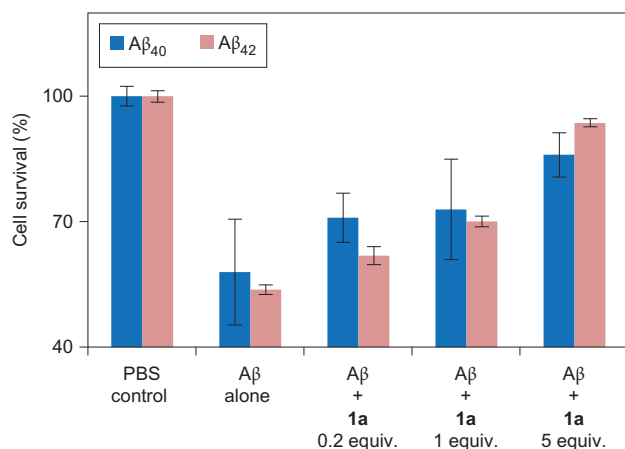


**Figure 4 | Effect of ABSM 1a on Aβ<sub>40</sub> and Aβ<sub>42</sub> toxicity towards PC-12 cells.** Addition of Aβ decreases cell survival when PC-12 cells are cultured for 24 h with preincubated Aβ. Cell survival increases when cells are cultured for 24 h with a preincubated mixture of ABSM 1a and Aβ in 0.2, 1.0 and 5 molar ratios. Cell survival is given as a percentage relative to controls in which only PBS is added. The cell survival of the PBS controls is taken to be 100%. Error bars correspond to standard deviations of four sets of experiments. For experimental details, see Supplementary Information.

- 1 effect of ABSM 1a on the toxicity of Aβ<sub>40</sub> and Aβ<sub>42</sub>, because ABSM  
 2 1a exhibits the best inhibitory activity among those studied. We first  
 3 incubated Aβ monomers (5 μM) without ABSM 1a to allow Aβ  
 4 oligomers and fibrils to form. The resulting Aβ mixtures were  
 5 used directly in cell viability assays. These assays showed that the  
 6 Aβ<sub>40</sub> and Aβ<sub>42</sub> preincubated without ABSM 1a kill 42% and 46%  
 7 of the PC-12 cells, respectively, relative to controls in which the  
 8 cells are incubated in only phosphate-buffered saline (PBS) buffer  
 9 solutions (Fig. 4).  
 10 Cell viability assays further established that preincubation of Aβ  
 11 with ABSM 1a rescues the cells in a dose-dependent manner.  
 12 Preincubation of Aβ<sub>40</sub> and Aβ<sub>42</sub> with 0.2 equiv. of ABSM 1a

reduces the death of PC-12 to 29% and 38%, respectively, while pre-  
 incubation with 1.0 equiv. reduces cell death to 27% and 30% and  
 preincubation with 5 equiv. reduces cell death to 14% and 6%.  
 The rescue of these neuron-like cells by ABSM 1a suggests that  
 ABSMs may reduce the production of toxic amyloid oligomers or  
 bind the oligomers and reduce their toxicity.

## Discussion

ABSMs 1 provide a unique tool with which to elucidate the process  
 of amyloid aggregation. Although many of the details of amyloid  
 aggregation remain unclear, nucleation-dependent polymerization,  
 where seeding to form a β-structured nucleus is the rate-determin-  
 ing step, is widely accepted<sup>1,22</sup>. Based on nucleation-dependent  
 polymerization, we propose a model for the potent inhibition of  
 Aβ aggregation by ABSM 1a. In this model, ABSM 1a binds early  
 β-structured oligomers and blocks Aβ nucleation (Fig. 5a).  
 Without ABSM 1a, the unstructured monomer forms β-structured  
 oligomers, which, in the rate-determining step, go on to form a  
 β-structured nucleus that ultimately assembles to form cross-β  
 fibrils. The solid line in Fig. 5a illustrates this pathway. ABSM 1a  
 creates a new aggregation pathway for the early β-structured oligomers.  
 In this pathway, ABSM 1a binds the β-structured oligomers to  
 form Aβ-oligomer-ABSM-1a complexes and blocks the Aβ oligomer-  
 to-nucleus transition. The dashed line in Fig. 5a illustrates this  
 pathway.

It is significant that ABSM 1a substantially delays the aggregation  
 of Aβ at sub-stoichiometric concentrations (as low as 1 μM),  
 for example, 0.05 equiv. of ABSM 1a per equivalent of Aβ  
 (Supplementary Fig. S2), while simple linear peptide fragments  
 derived from Aβ generally show substantial inhibitory effects at  
 stoichiometric or greater concentrations<sup>33,34</sup>. This observation  
 suggests that ABSM 1a binds a larger oligomer, not the monomer  
 or a smaller oligomer such as a dimer, trimer or tetramer. ABSM  
 1a binds the early β-structured oligomers more strongly than the  
 unstructured monomers bind oligomers, because the recognition  
 β-strand of ABSM 1a is preorganized. This preorganization there-  
 fore promotes the formation of Aβ-oligomer-ABSM-1a complexes.  
 The complexation may occur through edge-to-edge interactions

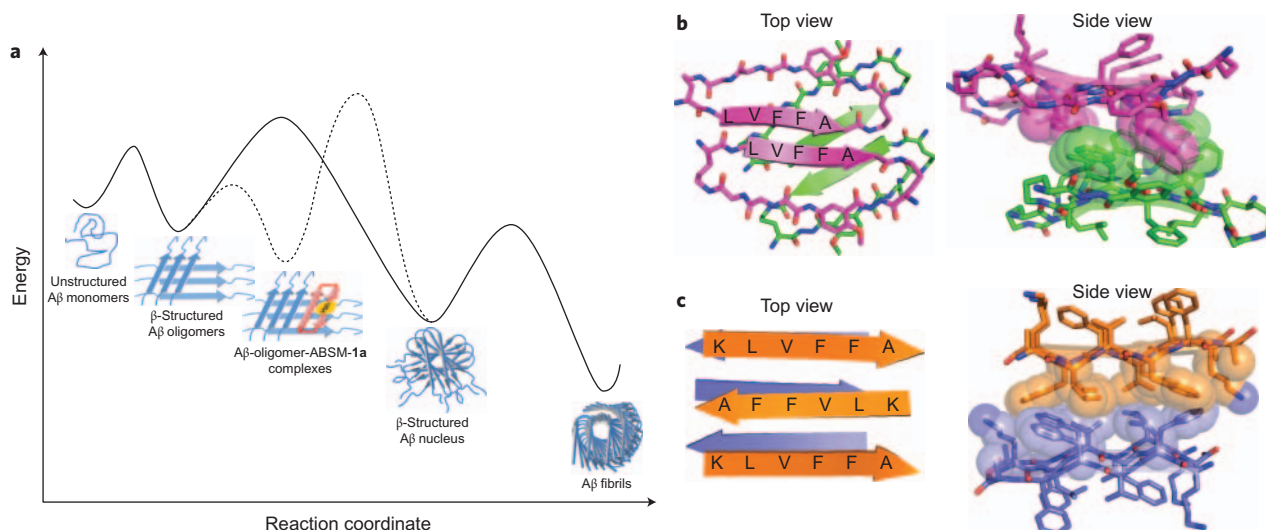


**Figure 5 | β-Sheet interactions of Aβ peptides and ABSM 1a.** **a**, Proposed model of inhibition of Aβ aggregation by ABSM 1a. The solid curve corresponds to a pathway in which Aβ aggregates without ABSM 1a. The dashed curve corresponds to an alternative pathway in which ABSM 1a inhibits Aβ aggregation by binding Aβ oligomers. **b**, Crystal structure of a macrocyclic peptide containing pentapeptide sequence LVFFA<sup>17</sup> (PDB ID: 3Q9H). The magenta and green structures correspond to parallel and antiparallel β-sheet dimers formed by the macrocyclic peptide. The side view shows hydrophobic contacts formed between the parallel and antiparallel β-sheet dimers. **c**, Crystal structure of the linear peptide KLVFFA<sup>35</sup> (PDB ID: 3OW9). The orange and purple structures correspond to different layers within the crystal structure. The side view shows hydrophobic contacts between the layers.

1 between the hydrogen-bonding edge of ABSM **1a** and exposed  
 2 hydrogen-bonding groups of the A $\beta$  oligomers, and through  
 3 face-to-face hydrophobic interactions between ABSM **1a** and the  
 4 hydrophobic surfaces of the A $\beta$  oligomers. These types of inter-  
 5 actions should take place between the hydrophobic sequence  
 6 A $\beta$ <sub>17–21</sub> of ABSM **1a** and that of the A $\beta$  oligomers, as observed in  
 7 the amyloid-related oligomers containing the pentapeptide  
 8 sequence LVFFA shown in Fig. 5b and the amyloid-like fibrils  
 9 from the hexapeptide KLVFFA shown in Fig. 5c. Similar inter-  
 10 actions should also occur in the interactions of other ABSMs with  
 11 their parent amyloidogenic peptides and proteins. The stabilization  
 12 of these complexes creates a higher energy barrier to formation of  
 13 the  $\beta$ -structured nucleus and thus delays or halts fibril formation.  
 14 Because ABSM **1a** cannot sequester all of the equilibrating A $\beta$  oli-  
 15 gomers, the A $\beta$  monomers and oligomers eventually succumb to  
 16 thermodynamics and form A $\beta$  fibrils.

17 The X-ray crystallographic structure of ABSM **1r** may provide  
 18 insights not only into the stabilization of the dimerization and  
 19 higher-order supramolecular assembly of ABSMs, but also into  
 20 the stabilization and structure of intermediates formed during  
 21 amyloid aggregation. The hydrophobic contacts formed by the Ile,  
 22 Leu and Val at positions 3, 5 and 7 of ABSM **1r** are akin to the  
 23 steric zipper of amyloid-like fibrils formed by fragments A $\beta$ <sub>16–21</sub>,  
 24 A $\beta$ <sub>30–35</sub>, A $\beta$ <sub>35–40</sub> and A $\beta$ <sub>37–42</sub> (refs 10 and 35). Both the layered  
 25 crystal structure of ABSM **1r** and the amyloid-like fibrils are stabil-  
 26 ized by hydrophobic contacts. These observations suggest that max-  
 27 imization of both hydrophobic contact and hydrogen bonding is key  
 28 to stabilizing not only amyloid fibrils but also transient amyloid  
 29 oligomers<sup>36</sup>.

## 30 Conclusion

31 The ABSMs **1** described herein provide a single platform with which  
 32 to display a variety of amyloidogenic heptapeptide  $\beta$ -strands and  
 33 provide a rational design for inhibitors to control amyloid aggrega-  
 34 tion. X-ray crystallographic and <sup>1</sup>H NMR studies validate that the  
 35 design of ABSMs **1**—including cyclicality, Hao template, two <sup>o</sup>Orn  
 36  $\beta$ -turn mimics and paired side chains—promotes the formation  
 37 of  $\beta$ -sheets in which the folding is largely independent of the  
 38 amino-acid sequence.

39 ABSMs **1** can be tailored to inhibit the aggregation of different  
 40 amyloid proteins. The inhibition of A $\beta$ , h $\beta$ <sub>2</sub>M and h $\alpha$ Syn<sub>1–100</sub>  
 41 aggregation by ABSMs **1** indicates that ABSMs containing one  
 42 hydrogen-bonding edge and one blocking edge are an effective  
 43 design for inhibitors of amyloid aggregation. The ability of  
 44 ABSMs **1a**, **1m** and **1o** to inhibit amyloid aggregation and to detox-  
 45 ify amyloid aggregates suggests the potential for therapeutic appli-  
 46 cations in amyloid-related diseases.

## 47 Materials and methods

48 Synthetic A $\beta$ <sub>40</sub> was purchased from GL Biochem (Shanghai). A $\beta$ <sub>42</sub>, h $\beta$ <sub>2</sub>M and  
 49 h $\alpha$ Syn<sub>1–100</sub> were expressed in *Escherichia coli* (for details, see Supplementary  
 50 Information). ABSMs **1** were synthesized as described above (for details, see  
 51 Supplementary Information). <sup>1</sup>H NMR, 2D TOCSY and 2D ROESY experiments  
 52 with ABSMs **1** were performed in D<sub>2</sub>O with DSA as an internal standard at  
 53 500 MHz and 298 K (for details, see Supplementary Information). Crystallization,  
 54 data collection and structure determination for the ABSM **1r** are described in the  
 55 Supplementary Information. ThT fluorescence assays and TEM studies of A $\beta$ , h $\beta$ <sub>2</sub>M  
 56 and h $\alpha$ Syn<sub>1–100</sub> aggregation with ABSMs **1a**, **1m** and **1o** are described in the  
 57 Supplementary Information. Cell viability assays to establish the toxicity of ABSMs  
 58 **1a**, **1m** and **1o** towards HeLa, HEK-293 and PC-12 cells are also described in the  
 59 Supplementary Information.

60 Received 26 March 2012; accepted 12 July 2012;

61 published online XX XX 2012

## 62 References

63 1. Chiti, F. & Dobson, C. M. Protein misfolding, functional amyloid, and human  
 64 disease. *Annu. Rev. Biochem.* **75**, 333–366 (2006).

2. Aguzzi, A. & O'Connor, T. Protein aggregation diseases: pathogenicity and  
 therapeutic perspectives. *Nature Rev. Drug. Discov.* **9**, 237–248 (2010). 66
3. Bartolini, M. & Andrisano, V. Strategies for the inhibition of protein aggregation  
 in human diseases. *ChemBioChem* **11**, 1018–1035 (2010). 67
4. Greenwald, J. & Riek, R. Biology of amyloid: structure, function, and regulation. 68  
*Structure* **18**, 1244–1260 (2010). 70
5. Tycko, R. Solid-state NMR studies of amyloid fibril structure. *Annu. Rev. Phys.*  
*Chem.* **62**, 279–299 (2011). 71
6. Eichner, T. & Radford, S. E. A diversity of assembly mechanisms of a generic  
 amyloid fold. *Mol. Cell* **43**, 8–18 (2011). 73
7. Lopez de la Paz, M. & Serrano, L. Sequence determinants of amyloid fibril  
 formation. *Proc. Natl Acad. Sci. USA* **101**, 87–92 (2004). 75
8. Goldschmidt, L., Teng, P. K., Riek, R. & Eisenberg, D. Identifying the amylo-  
 me, proteins capable of forming amyloid-like fibrils. *Proc. Natl Acad. Sci. USA* **107**,  
 3487–3492 (2010). 77
9. Nelson, R. *et al.* Structure of the cross- $\beta$  spine of amyloid-like fibrils. *Nature* **435**,  
 773–778 (2005). 81
10. Sawaya, M. R. *et al.* Atomic structures of amyloid cross- $\beta$  spines reveal varied  
 steric zippers. *Nature* **447**, 453–457 (2007). 82
11. Conway, K. A. *et al.* Acceleration of oligomerization, not fibrillization, is a shared  
 property of both  $\alpha$ -synuclein mutations linked to early-onset Parkinson's  
 disease: implications for pathogenesis and therapy. *Proc. Natl Acad. Sci. USA* **97**,  
 571–576 (2000). 84
12. Lashuel, H. A., Hartley, D., Petre, B. M., Walz, T. & Lansbury, P. T.  
 Neurodegenerative disease: amyloid pores from pathogenic mutations. *Nature*  
**418**, 291–291 (2002). 88
13. Chimon, S. *et al.* Evidence of fibril-like  $\beta$ -sheet structures in a neurotoxic  
 amyloid intermediate of Alzheimer's  $\beta$ -amyloid. *Nature Struct. Mol. Biol.* **14**,  
 1157–1164 (2007). 91
14. Bernstein, S. L. *et al.* Amyloid- $\beta$  protein oligomerization and the importance of  
 tetramers and dodecamers in the aetiology of Alzheimer's disease. *Nature Chem.*  
**1**, 326–331 (2009). 95
15. Ono, K., Condrón, M. M. & Teplow D. B. Structure–neurotoxicity relationships  
 of amyloid  $\beta$ -protein oligomers. *Proc. Natl Acad. Sci. USA* **106**,  
 14745–14750 (2009). 97
16. Woods, R. J. *et al.* Cyclic modular  $\beta$ -sheets. *J. Am. Chem. Soc.* **129**,  
 2548–2558 (2007). 100
17. Liu, C. *et al.* Characteristics of amyloid-related oligomers revealed by crystal  
 structures of macrocyclic  $\beta$ -sheet mimics. *J. Am. Chem. Soc.* **133**,  
 6736–6744 (2011). 102
18. Zheng, J. *et al.* Macrocyclic  $\beta$ -sheet peptides that inhibit the aggregation of a  
 tau-protein-derived hexapeptide. *J. Am. Chem. Soc.* **133**, 3144–3157 (2011). 106
19. Gellman, S. H. Minimal model systems for  $\beta$ -sheet secondary structure in  
 proteins. *Curr. Opin. Chem. Biol.* **2**, 717–725 (1998). 107
20. Nowick, J. S. *et al.* An unnatural amino acid that mimics a tripeptide  $\beta$ -strand  
 and forms  $\beta$ -sheetlike hydrogen-bonded dimers. *J. Am. Chem. Soc.* **122**,  
 7654–7661 (2000). 110
21. Nowick, J. S. & Brower, J. O. A new turn structure for the formation of  
 $\beta$ -hairpins in peptides. *J. Am. Chem. Soc.* **125**, 876–877 (2003). 112
22. Finder, V. H. & Glockshuber, R. Amyloid- $\beta$  aggregation. *Neurodegen. Dis.* **4**,  
 13–27 (2007). 114
23. Walsh, P., Simonetti, K. & Sharpe, S. Core structure of amyloid fibrils  
 formed by residues 106–126 of the human prion protein. *Structure* **17**,  
 417–426 (2009). 116
24. Friedhoff, P., von Bergen, M., Mandelkow, E.-M., Davies, P. & Mandelkow, E.  
 A nucleated assembly mechanism of Alzheimer paired helical filaments. *Proc.*  
*Natl Acad. Sci. USA* **95**, 15712–15717 (1998). 120
25. Platt, G. W., Routledge, K. E., Homans, S. W. & Radford, S. E. Fibril growth  
 kinetics reveal a region of  $\beta$ <sub>2</sub>-microglobulin important for nucleation and  
 elongation of aggregation. *J. Mol. Biol.* **378**, 251–263 (2008). 122
26. Vilar, M. *et al.* The fold of  $\alpha$ -synuclein fibrils. *Proc. Natl Acad. Sci. USA* **105**,  
 8637–8642 (2008). 125
27. Luca, S., Yau, W.-M., Leapman, R. & Tycko, R. Peptide conformation and  
 supramolecular organization in amylin fibrils: constraints from solid-state NMR. 127  
*Biochemistry* **46**, 13505–13522 (2007). 129
28. Cheng, P.-N. & Nowick, J. S. Giant macrolactams based on  $\beta$ -sheet peptides. 130  
*J. Org. Chem.* **76**, 3166–3173 (2011). 131
29. Yan, L.-M., Velkova, A., Taterek-Nossol, M., Andreetto, E. & Kapurniotu, A. 132  
 IAPP mimic blocks A $\beta$  cytotoxic self-assembly: cross-suppression of amyloid  
 toxicity of A $\beta$  and IAPP suggests a molecular link between Alzheimer's disease 134  
 and type II diabetes. *Angew. Chem. Int. Ed.* **46**, 1246–1252 (2007). 135
30. Seeliger, J. *et al.* Cross-amyloid interaction of A $\beta$  and IAPP at lipid membranes. 136  
*Angew. Chem. Int. Ed.* **51**, 679–683 (2012). 137
31. Ma, B. & Nussinov, R. Selective molecular recognition in amyloid growth and  
 transmission and cross-species barriers. *J. Mol. Biol.* <http://doi.org/10.1016/j.jmb.2011.11.023> (2012). 139
32. Miller, Y., Ma, B. & Nussinov, R. Polymorphism in Alzheimer A $\beta$  amyloid 141  
 organization reflects conformational selection in a rugged energy landscape. 142  
*Chem. Rev.* **110**, 4820–4838 (2010). 143

Q7

Q8  
Q9

Q9

- 1 33. Stains, C. I., Mondal, K. & Ghosh, I. Molecules that target beta-amyloid.  
2 *ChemMedChem* **2**, 1674–1692 (2007).  
3 34. Sciarretta, K. L., Gordon, D. J. & Meredith, S. C. Peptide-based inhibitors of  
4 amyloid assembly. *Methods Enzymol.* **413**, 273–312 (2006).  
5 35. Colletier, J.-P. *et al.* Molecular basis for amyloid- $\beta$  polymorphism. *Proc. Natl*  
6 *Acad. Sci. USA* **108**, 16938–16943 (2011).  
7 36. Laganowsky, A. *et al.* Atomic view of a toxic amyloid small oligomer. *Science*  
8 **335**, 1228–1231 (2012).

### 9 Acknowledgements

- 10 The authors acknowledge support from the NIH (5R01 GM049076, 1R01 GM097562  
11 and 1R01 AG029430), the NSF (CHE-1112188, CHE-0750523 and MCB-0445429) and  
12 HHMI. The authors also thank A. Berk and D. Guo for help with tissue culture  
23 experiments, and S. Blum for suggestions for Fig. 5a.

### Author contributions

P.-N.C., C.L., D.E. and J.S.N. designed the research. P.-N.C., C.L. and M.Z. performed the  
15 research. P.-N.C., C.L., M.Z., D.E. and J.S.N. analysed the data. P.-N.C., C.L., M.Z., D.E. and  
16 J.S.N. wrote the paper. 17

Q10

### Additional information

Supplementary information and chemical compound information are available in the  
19 online version of the paper. Reprints and permission information is available online at  
20 <http://www.nature.com/reprints>. Correspondence and requests for materials should be  
21 addressed to D.E. and J.S.N. 22

### Competing financial interests

The authors declare no competing financial interests. 23  
24

Publisher: Nature

Journal: Nature Chemistry

Article number: nchem.1433

Author (s): Pin-Nan Chen *et al.*

Title of paper: Macrocyclic  $\beta$ -sheet mimics that antagonize protein aggregation and reduce amyloid toxicity

Query no.	Query	Response
1	Please check the title – this has been amended slightly to avoid the repetition of ‘amyloid’.	
2	In the abstract – please check that A $\beta$ has been expanded properly. I am not sure that ‘peptide’ should be included – please clarify.	
3	Please check that abstract is OK as amended	
4	HPLC expanded OK?	
5	Sentence beginning “The Ile” OK as amended?	
6	NOE expanded OK?	
7	Sentence beginning “X-ray” OK as amended?	
8	Please expand these acronyms	
9	Please provide updated information for ref 31	
10	The statement of equal contribution is now included as a footnote on the front page of this article. Please check	